

Fast and Accurate Tensor Completion with Tensor Trains: A System Identification Approach

Ching-Yun Ko¹, Kim Batselier¹, Wenjian Yu², Ngai Wong¹,

¹ The Department of Electrical and Electronic Engineering, The University of Hong Kong

² The Department of Computer Science and Technology, Tsinghua University

cyko@eee.hku.hk, kimb@eee.hku.hk, yu-wj@tsinghua.edu.cn, nwong@eee.hku.hk

Abstract

We propose a novel tensor completion approach by equating it to a system identification task. The key is to regard the coordinates and values of the known entries as inputs and outputs, respectively. By assuming a tensor train format initialized with low-rank tensor cores, the latter are iteratively identified via a simple alternating linear scheme to reduce residuals. Experiments verify the superiority of the proposed scheme in terms of both speed and accuracy, where a speedup of up to $23\times$ is observed compared to state-of-the-art tensor completion methods at a similar accuracy.

1 Introduction

Tensors are natural higher-order generalization of vectors and matrices. Considerable attention has recently been given to tensor arithmetic due to the development in tensor decomposition and its effectiveness in big data applications. Apart from its profound history in mathematics and physics, tensor algebra is being explored in engineering fields such as hyperspectral data recovery [Xing *et al.*, 2012], higher-order web link analysis [Kolda *et al.*, 2005], seismic data reconstruction [Kreimer and Sacchi, 2012], visual data recovery [Liu *et al.*, 2013; Gandy *et al.*, 2011], electronics design automation [Zhang *et al.*, 2017] and system identification [Batselier *et al.*, 2017]. Such wide applications of tensors are actually no surprise as tensors naturally represent real life multi-way data like images and videos. In this work, we solve the tensor completion problem using an innovative system identification idea. A novel algorithm is proposed that connects applications in the field of computer vision with regression tasks by applying a tensor train system identification approach to image in-painting and video completion tasks.

The tensor completion problem can be considered as a generalization of the matrix completion problem, which aims at estimating missing entries from partially revealed data. For example, grayscale images are matrices (two-way tensors) that are indexed by two spatial variables while color images are essentially three-way tensors with one additional color dimension. Grayscale and color videos are extensions of grayscale and color images by adding one temporal index.

Thus image/video recovery tasks are indeed tensor completion problems. Although one can always regard a tensor completion task as multiple matrices completion problems, state-of-the-art matrix completion algorithms such as [Cai *et al.*, 2010] have rather high computational costs and poor scalability. Moreover, the application of matrix completion methods to tensorial data overlooks a key insight in tensor completion: the low tensor-rank assumption [Liu *et al.*, 2013; Xu *et al.*, 2015; Kolda and Bader, 2009; Grasedyck *et al.*, 2015] inherent to the data. For example, videos are stitched frame by frame and each frame is an image. However, normally every two adjacent frames of a video are shot with a very short time interval, implying only limited changes are allowed between two adjacent video frames. Similarly, the values among neighbor pixels in an image usually vary slowly.

Most existing tensor completion methods are generalizations of matrices completion methods. Traditional matrix completion problems are generally translated into the construction of a structurally low-rank matrix \mathbf{E} that has the same observed entries, which is formulated as:

$$\min_{\mathbf{E}} \text{rank}(\mathbf{E}), \text{ s.t. } (\mathbf{E} - \mathbf{O})_{\Omega} = \mathbf{0}$$

where \mathbf{O} represents the observed matrix with zero filling at missing entries, and Ω is the mapping that specifies the location of known entries. Directly solving the above optimization problem is NP-hard, which results in extensive research on solving alternative formulations. Two popular candidates are to minimize the nuclear norm as the convex envelope of the matrix rank-operator [Candès and Recht, 2009; Chen, 2015], or to use a factorization method [Wen *et al.*, 2012] that decomposes the matrix \mathbf{E} as the product of two small matrices. The nuclear norm minimization idea has been generalized to tensor completion problems by unfolding the tensor along its k modes and summing over the nuclear norm of the resulting k matrices [Liu *et al.*, 2013; Collins and Cohen, 2012; Signoretto *et al.*, 2014]. Correspondingly, the factorization method has also been generalized to tensors [Xu *et al.*, 2015; Tan *et al.*, 2014]. Another way to tackle tensor completion is based on the tensor multi-rank and tubal rank [Kilmer *et al.*, 2013; Semerci *et al.*, 2014; Zhang *et al.*, 2014; Mu *et al.*, 2014; Zhou *et al.*, 2017], which are intrinsically defined on three-way tensors such as color images and grayscale videos. It is remarked that multi-rank and tubal rank inspired methods are only applicable when

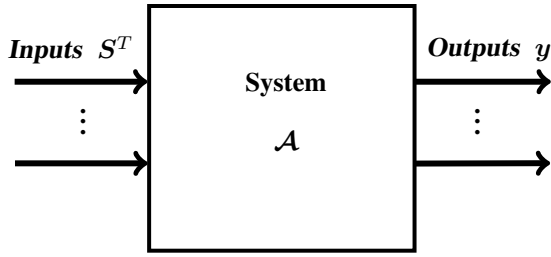


Figure 1: The unknown tensor \mathcal{A} in the tensor completion problem is interpreted as a dynamical system.

the data is compressible in a t-SVD representation. Methods that exploit other tensor formats including the tensor train format have also been proposed [Grasedyck *et al.*, 2015; Wang *et al.*, 2017]. Nonetheless, our method is fundamentally different as it relies on an alternative formulation of the tensor completion problem as a system identification task.

Tensor decompositions are playing an increasingly important role in compressing and processing data. Although the Canonical Polyadic (CP) and Tucker decompositions have found many applications, the tensor train decomposition and its applications are relatively unknown. Actually, the tensor train format has been successfully applied to various applications in the field of engineering, including the identification of high-order multi-input multi-output Volterra systems [Batselier *et al.*, 2017]. Motivated by this success, we reformulate the tensor completion problem as a system identification problem as shown in Figure 1. The unknown completed tensor \mathcal{A} is thereby interpreted as the system to identify, while the observed inputs and outputs are the multi-indices of the known entries and the corresponding values, respectively. The tensor completion problem is then solved from the following optimization problem

$$\begin{aligned} \min_{\mathcal{A}} \quad & \|S^T \text{vec}(\mathcal{A}) - \mathbf{y}\|_2^2, \\ \text{s.t.} \quad & \text{TT-rank}(\mathcal{A}) = (R_1, R_2, \dots, R_d). \end{aligned}$$

The binary matrix S^T selects the known entries of $\text{vec}(\mathcal{A})$, where $\text{vec}(\mathcal{A})$ denotes the vectorization of the unknown completed tensor \mathcal{A} . The vector \mathbf{y} contains the values of the observed tensor entries. Minimizing $\|S^T \text{vec}(\mathcal{A}) - \mathbf{y}\|_2^2$ therefore enforces the requirement that the desired solution needs to have the same observed tensor entries. In order to regularize the problem, an additional low-rank constraint is added together with the requirement that the desired tensor is represented in the tensor train format, which will be explained in Section 3. The above problem is solved using an iterative method called the alternating linear scheme. The main contributions of this article are:

- The tensor completion problem is rephrased and solved as a system identification problem, allowing system identification techniques and new insights.
- Initialization methods are designed to speed up the convergence, and an alternating linear scheme is employed to update the tensor train cores.

To the best of our knowledge, this is the first time that the

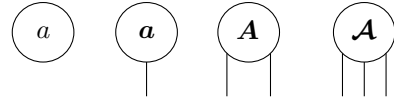


Figure 2: Graphical depiction of a scalar a , vector \mathbf{a} , matrix \mathbf{A} and 3-way tensor \mathcal{A} .

tensor completion problem is interpreted as a system identification problem. The efficacy of the proposed algorithm is demonstrated by extensive numerical experiments.

The outline of the article is as follows. We briefly introduce some necessary tensor and tensor train preliminaries in Section 2. The proposed tensor train completion model is formed and discussed in Section 3. Details on the initialization and updating scheme of the proposed algorithm are given in Section 4. Numerical experiments comparing our proposed algorithm with state-of-the-art methods are given in Section 5. Conclusions are drawn in Section 6.

2 Preliminaries

Tensors are high-dimensional arrays that generalize vectors and matrices. A d -way or d -order tensor $\mathcal{A} \in \mathbb{R}^{I_1 \times I_2 \times \dots \times I_d}$ is an array where each entry is indexed by d indices i_1, i_2, \dots, i_d . We use the convention $1 \leq i_k \leq I_k$ for $k = 1, \dots, d$. MATLAB notation is used to denote entries of tensors. In this paper, boldface capital calligraphic letters $\mathcal{A}, \mathcal{B}, \dots$ are used to denote tensors, boldface capital letters $\mathbf{A}, \mathbf{B}, \dots$ denote matrices, boldface letters $\mathbf{a}, \mathbf{b}, \dots$ denote vectors, and Roman letters a, b, \dots denote scalars. A set of d tensors, like that of a tensor train, is denoted as $\mathcal{A}^{(1)}, \mathcal{A}^{(2)}, \dots, \mathcal{A}^{(d)}$. To facilitate understanding of tensor representations and operations, a graphical depiction of scalars, vectors, matrices, and tensors is introduced in Figure 2, where each node represents a tensor and the number of free edges on each node represents its order. For example, matrices are 2-way tensors, and thus are represented by nodes with two unconnected edges. We now give a brief description of some required tensor operations. The generalization of the matrix-matrix multiplication to tensors involves a multiplication of a matrix with a d -way tensor along one of its d modes.

Definition 2.1 ([Kolda and Bader, 2009, p. 460]) *The k -mode product of a tensor $\mathcal{A} \in \mathbb{R}^{I_1 \times \dots \times I_d}$ with a matrix $\mathbf{U} \in \mathbb{R}^{J \times I_k}$ is denoted $\mathcal{B} = \mathcal{A} \times_k \mathbf{U}$ and defined by*

$$\mathcal{B}(i_1, \dots, i_{k-1}, j, i_{k+1}, \dots, i_d) = \sum_{i_k=1}^{I_k} \mathbf{U}(j, i_k) \mathcal{A}(i_1, \dots, i_{k-1}, i_k, i_{k+1}, \dots, i_d),$$

where $\mathcal{B} \in \mathbb{R}^{I_1 \times \dots \times I_{k-1} \times J \times I_{k+1} \times \dots \times I_d}$.

The proposed method also requires the knowledge of the matrix Khatri-Rao product and Kronecker product, which play crucial roles in the construction of the input matrix \mathbf{S} .

Definition 2.2 *If $\mathbf{A} \in \mathbb{R}^{N_1 \times M_1}$ and $\mathbf{C} \in \mathbb{R}^{N_2 \times M_2}$, then*

their Kronecker product $\mathbf{A} \otimes \mathbf{C}$ is the $N_1 N_2 \times M_1 M_1$ matrix

$$\begin{pmatrix} \mathbf{A}(1, 1)\mathbf{C} & \cdots & \mathbf{A}(1, M_1)\mathbf{C} \\ \vdots & \ddots & \vdots \\ \mathbf{A}(N_1, 1)\mathbf{C} & \cdots & \mathbf{A}(N_1, M_1)\mathbf{C} \end{pmatrix}.$$

Definition 2.3 If $\mathbf{A} \in \mathbb{R}^{N_1 \times M}$ and $\mathbf{C} \in \mathbb{R}^{N_2 \times M}$, then their Khatri-Rao product $\mathbf{A} \odot \mathbf{C}$ is the $N_1 N_2 \times M$ matrix

$$(\mathbf{A}(:, 1) \otimes \mathbf{C}(:, 1) \quad \cdots \quad \mathbf{A}(:, M) \otimes \mathbf{C}(:, M)).$$

The vectorization $\text{vec}(\mathcal{A})$ of a tensor \mathcal{A} is the vector obtained from concatenating all tensor entries into one column vector. More details on these tensor operations can be found in [Kolda and Bader, 2009, p. 459]. A tensor train (TT) represents a vector \mathbf{a} of length $I_1 I_2 \cdots I_d$ by a set of 3-way tensors $\mathcal{A}^{(1)}, \mathcal{A}^{(2)}, \dots, \mathcal{A}^{(d)}$, where each tensor $\mathcal{A}^{(k)} \in \mathbb{R}^{R_k \times I_k \times R_{k+1}}$ ($k = 1, \dots, d$) is called a tensor train core. Note that $R_{d+1} = R_1$, which we explain along with the formal definition of a tensor train. A graphical representation of a tensor train is shown in Figure 3. The mapping between the index of the vector \mathbf{a} and the multi-index of the corresponding tensor is bijective: every vector entry $\mathbf{a}(i)$ corresponds to one and only one multi-index $[i_1, i_2, \dots, i_d]$, and vice versa. Herein we adopt the mapping convention

$$i = i_1 + \sum_{k=2}^d (i_k - 1) \prod_{p=1}^{k-1} I_p, \quad (1)$$

to convert the multi-index $[i_1, i_2, \dots, i_d]$ into the single-index i . We now give the formal definition of a tensor train.

Definition 2.4 A tensor train of a vector $\mathbf{a} \in \mathbb{R}^{I_1 I_2 \cdots I_d}$ is defined as the set of d 3-way tensors $\mathcal{A}^{(1)}, \dots, \mathcal{A}^{(d)}$ such that $\mathbf{a}(i)$ equals

$$\sum_{r_1, \dots, r_{d+1}} \mathcal{A}^{(1)}(r_1, i_1, r_2) \mathcal{A}^{(2)}(r_2, i_2, r_3) \cdots \mathcal{A}^{(d)}(r_d, i_d, r_{d+1}), \quad (2)$$

where i is related to $[i_1, i_2, \dots, i_d]$ via (1) and r_1, r_2, \dots, r_{d+1} are auxiliary indices that are summed over.

The summations over the auxiliary indices are represented in Figure 3 by the connected edges between the different nodes. The dimensions R_1, R_2, \dots, R_{d+1} of these auxiliary indices are called the tensor train ranks (TT-ranks). The condition $R_1 = R_{d+1}$ ensures that the summation in (2) results in a scalar. Throughout this article we further assume that $R_1 = R_{d+1} = 1$. Upper bounds on the remaining tensor train ranks are derived in [Oseledets, 2011]. Using a tensor train format can reduce the number of elements to store a tensor significantly. The storage of a tensor train of a d -way tensor $\mathcal{Z} \in \mathbb{R}^{I_1 \times I_2 \times \cdots \times I_d}$ requires approximately dIR^2 elements, where R is the maximum tensor train rank, compared to the conventional I^d storage requirement.

3 Tensor Train Completion Model

The proposed tensor completion method intrinsically relies on solving an underdetermined linear system under a low

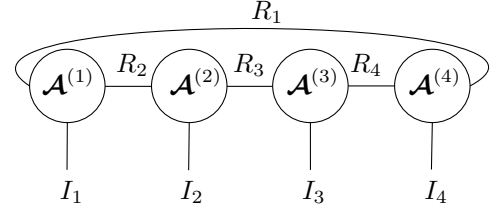


Figure 3: Graphical depiction of a tensor train that consists of four 3-way tensors $\mathcal{A}^{(1)}, \dots, \mathcal{A}^{(4)}$.

TT-rank constraint. For a given set of N multi-indices $[i_1, i_2, \dots, i_d]$ and a corresponding vector of observed tensor entries $\mathbf{y} \in \mathbb{R}^N$, the goal is to obtain a tensor $\mathcal{A} \in \mathbb{R}^{I_1 \times \cdots \times I_d}$ that contains the same tensor entries. Equivalently, we form the optimization problem

$$\min_{\mathcal{A}} \|\mathbf{S}^T \text{vec}(\mathcal{A}) - \mathbf{y}\|_2^2, \quad (3)$$

$$\text{s.t. TT-rank}(\mathcal{A}) = (R_1, R_2, \dots, R_d), \quad (4)$$

where $\mathbf{S}^T \in \mathbb{R}^{N \times I_1 I_2 I_3 \cdots I_d}$ is the row selection matrix corresponding with the known multi-indices. In other words, we want $\mathbf{S}^T \text{vec}(\mathcal{A}) \in \mathbb{R}^{N \times 1}$ to be as close as possible to the observed entries \mathbf{y} , under the constraint that $\text{vec}(\mathcal{A})$ has a low-rank tensor train representation. We stress that the tensor \mathcal{A} is never computed explicitly in the proposed algorithm but is stored in its tensor train format instead. This is possible by exploiting the fact that \mathbf{S} can be written as the Khatri-Rao product of d smaller binary matrices

$$\mathbf{S} = \mathbf{S}^{(d)} \odot \mathbf{S}^{(d-1)} \odot \cdots \odot \mathbf{S}^{(1)}. \quad (5)$$

This decomposition of \mathbf{S} follows from the following definition.

Definition 3.1 For a tensor entry $\mathcal{A}(i_1, i_2, \dots, i_d)$, the selection vector $\mathbf{s}_{[i_1, i_2, \dots, i_d]}$ is defined as

$$\mathbf{s}_{[i_1, i_2, \dots, i_d]} := \mathbf{e}_{i_d} \otimes \cdots \otimes \mathbf{e}_{i_2} \otimes \mathbf{e}_{i_1}, \quad (6)$$

where $\mathbf{e}_{i_k} \in \mathbb{R}^{I_k}$ ($k = 1, 2, \dots, d$) is the i_k th standard basis vector.

One can verify that

$$\mathbf{s}_{[i_1, i_2, \dots, i_d]}^T \text{vec}(\mathcal{A}) = \mathcal{A}(i_1, i_2, \dots, i_d).$$

Note that the order of the Kronecker products is reversed to be consistent with the index mapping (1). Equation (5) follows from the concatenation of the selection vectors for each known multi-index.

Example 1 We use a small example to illustrate Definition 3.1. Consider a $3 \times 4 \times 2$ tensor \mathcal{A} with only 3 of the entries observed. The multi-indices z_1, z_2, z_3 of the three observed entries are

$$z_1 = [2, 1, 2], z_2 = [1, 3, 1], z_3 = [3, 4, 2].$$

The corresponding selection vectors are then given by

$$\mathbf{s}_{z_1} = \mathbf{e}_2 \otimes \mathbf{e}_1 \otimes \mathbf{e}_2,$$

$$\mathbf{s}_{z_2} = \mathbf{e}_1 \otimes \mathbf{e}_3 \otimes \mathbf{e}_1,$$

$$\mathbf{s}_{z_3} = \mathbf{e}_2 \otimes \mathbf{e}_4 \otimes \mathbf{e}_3.$$

In our system identification interpretation, the d matrices $\mathbf{S}^{(1)}, \mathbf{S}^{(2)}, \dots, \mathbf{S}^{(d)}$ from (5) act as the inputs to the unknown system. We reuse the above example to demonstrate the construction of these matrices.

Example 2 Consider the known tensor entries in Example 1. We concatenate the first index components of $\mathbf{s}_{z_1}, \mathbf{s}_{z_2}, \mathbf{s}_{z_3}$ into $\mathbf{S}^{(1)}$ as

$$\mathbf{S}^{(1)} = (\mathbf{e}_2 \quad \mathbf{e}_1 \quad \mathbf{e}_3) \in \mathbb{R}^{3 \times 3}.$$

Similarly, $\mathbf{S}^{(2)}, \mathbf{S}^{(3)}$ are constructed from the concatenations of the second and third components, respectively

$$\begin{aligned} \mathbf{S}^{(2)} &= (\mathbf{e}_1 \quad \mathbf{e}_3 \quad \mathbf{e}_4) \in \mathbb{R}^{4 \times 3}, \\ \mathbf{S}^{(3)} &= (\mathbf{e}_2 \quad \mathbf{e}_1 \quad \mathbf{e}_2) \in \mathbb{R}^{2 \times 3}. \end{aligned}$$

The output in our system identification interpretation is the vector of N observed tensor entries

$$\mathbf{y} = (y_1, y_2, \dots, y_N)^T,$$

where typically $N \ll I_1 I_2 \dots I_d$.

4 Tensor Train Completion Algorithm

4.1 Tensor Train Initialization

The proposed tensor completion algorithm solves (3) iteratively using an alternating linear scheme (ALS) [Batselier *et al.*, 2017]. Starting from an initial guess for the tensor train of $\text{vec}(\mathcal{A})$, the ALS updates each tensor train core for a predefined number of iterations or until convergence. Each tensor train core update is achieved by solving a relative small (compared to the original tensor size) least squares problem. A good initial guess is therefore of crucial importance to speed up convergence. Through extensive tests, we observed that the following heuristical initialization method is effective in terms of convergence speed.

Suppose $\mathcal{V} \in \mathbb{R}^{I_1 \times I_2 \times \dots \times I_d}$ is a tensor with missing entries. Before converting \mathcal{V} into a tensor train, the goal is to fill up the missing entries using information from the observed entries through two interpolation steps. First, each dimension of the tensor \mathcal{V} is resized by a factor k using a box-shaped interpolation kernel. The resulting tensor is denoted $\mathcal{W} \in \mathbb{R}^{\lfloor \frac{I_1}{k} \rfloor \times \lfloor \frac{I_2}{k} \rfloor \times \dots \times \lfloor \frac{I_d}{k} \rfloor}$ and its entries are then used to construct a tensor of the original size $\mathcal{X} \in \mathbb{R}^{I_1 \times I_2 \times \dots \times I_d}$ through cubic kernel interpolation. Alternatively, one can use max or average pooling together with interpolation to achieve a similar effect. Finally, a tensor train with given TT-ranks is computed from tensor \mathcal{X} by a modified version of the TT-SVD algorithm [Oseledets, 2011, p. 2301]. The TT-SVD algorithm decomposes a tensor to its tensor train format by consecutive reshapings and singular value decomposition (SVD). The modification is made in line 5 of the TT-SVD algorithm, where instead of using the original truncation parameter δ , each SVD is truncated to the prescribed TT-rank R_2, \dots, R_d .

4.2 Alternating Linear Scheme

We now derive the least squares problem for updating each tensor train core during the ALS. The main motivation for

solving (3) in a tensor train form is the reduction in computational cost. Indeed, we will show how solving (3) for a d -way tensor \mathcal{A} with dimensions $I_1 = \dots = I_d = I$ in tensor train form using the ALS has a computational cost of $O(N(R^2 I)^2)$ flops, where R is the maximal TT-rank. In vector form the computational cost would take approximately $O(N^2 I^d)$ flops. In addition, by specifying small TT-ranks one effectively regularizes the problem since the underdetermined system $\mathbf{S}^T \text{vec}(\mathcal{A}) = \mathbf{y}$ will typically have an infinite number of solutions. In what follows, $\mathbf{s}_l^{(k)} \in \mathbb{R}^{I_k \times 1}$ ($l = 1, 2, \dots, N$) denotes the l -th column of the matrix $\mathbf{S}^{(k)}$. We further define the following useful auxiliary notations

$$\begin{aligned} \mathbf{a}_{<k,l}^T &:= (\mathcal{A}^{(1)} \times_2 \mathbf{s}_l^{(1)T}) \dots (\mathcal{A}^{(k-1)} \times_2 \mathbf{s}_l^{(k-1)T}) \in \mathbb{R}^{R_k}, \\ \mathbf{a}_{>k,l} &:= (\mathcal{A}^{(k+1)} \times_2 \mathbf{s}_l^{(k+1)T}) \dots (\mathcal{A}^{(d)} \times_2 \mathbf{s}_l^{(d)T}) \in \mathbb{R}^{R_{k+1}}, \end{aligned}$$

for $k = 2, \dots, d-1$. Per definition $\mathbf{a}_{<1,l} = \mathbf{a}_{>d,l} = 1$. The l -th observed entry $y(l)$ can then be written as

$$y(l) = (\mathbf{a}_{>k,l}^T \otimes \mathbf{s}_l^{(k)T} \otimes \mathbf{a}_{<k,l}) \text{vec}(\mathcal{A}^{(k)}). \quad (7)$$

The proof of equation (7) resembles that in [Batselier *et al.*, 2017, Theorem 4.1]. Writing out (7) for all N observed entries results in the following linear system

$$\mathbf{y} = \begin{pmatrix} \mathbf{a}_{>k,1}^T \otimes \mathbf{s}_1^{(k)T} \otimes \mathbf{a}_{<k,1} \\ \mathbf{a}_{>k,2}^T \otimes \mathbf{s}_2^{(k)T} \otimes \mathbf{a}_{<k,2} \\ \vdots \\ \mathbf{a}_{>k,N}^T \otimes \mathbf{s}_N^{(k)T} \otimes \mathbf{a}_{<k,N} \end{pmatrix} \text{vec}(\mathcal{A}^{(k)}), \quad (8)$$

where the matrix size is $N \times R_k I_k R_{k+1}$. We now add the constraint that the TT-ranks R_k, R_{k+1} are chosen such that $N \gg R_k I_k R_{k+1}$. The computational cost for solving (8) is then $O(N(R_k I_k R_{k+1})^2)$ and results in a new estimate for the tensor train core $\mathcal{A}^{(k)}$. The key idea of the ALS is to solve (8) for varying values of k in a “sweeping” fashion, starting from the leftmost tensor train core $\mathcal{A}^{(1)}$ to the rightmost $\mathcal{A}^{(d)}$ and then back from the rightmost to the leftmost. The numerical stability of the ALS algorithm is guaranteed through an orthogonalization step, cf. [Holtz *et al.*, 2012, p. A701] and [Batselier *et al.*, 2017].

4.3 Tensor Train Completion Algorithm

The pseudocode of the proposed tensor train completion (TTC) algorithm is given as Algorithm 1. First, d binary input matrices $\mathbf{S}^{(1)}, \mathbf{S}^{(2)}, \dots, \mathbf{S}^{(d)}$ are constructed as specified in Section 3. The tensor train with specified TT-ranks is then initialized according to Section 4.1. The ALS is then applied to update the tensor train cores one by one in a sweeping fashion. One can update the tensor train cores for a fixed amount of sweeps or until the residual falls below a certain threshold. Algorithm 1 computes a tensor train representation $\mathcal{A}^{(1)}, \dots, \mathcal{A}^{(d)}$ of the desired tensor \mathcal{A} . Depending on the application one can either choose to keep the result in tensor train form or compute the full tensor \mathcal{A} by contracting the tensor train over cores as in Figure 3.

Algorithm 1 Tensor completion in tensor train form (TTC)

Input: d -way multi-indices z_1, \dots, z_N of N known entries and their corresponding values $\mathbf{y}(1), \dots, \mathbf{y}(N)$, TT ranks R_2, \dots, R_d .

Output: Completed tensor \mathcal{A} in tensor train form $\mathcal{A}^{(1)}, \dots, \mathcal{A}^{(d)}$.

```

1: Construct binary input matrices  $\mathbf{S}^{(1)}, \mathbf{S}^{(2)}, \dots, \mathbf{S}^{(d)}$  as
   specified in Section 3
2: Initialize the tensor train as specified in Section 4.1
3: while stopping criteria not satisfied do
4:   for  $k=1, \dots, d-1$  do
5:      $\text{vec}(\mathcal{A}^{(k)}) \leftarrow$  compute and solve equation (8)
6:      $\mathbf{A}_k \leftarrow \text{reshape}(\mathcal{A}^{(k)}, [R_k I_k, R_{k+1}])$ 
7:   end for
8:   for  $k=d, \dots, 2$  do
9:      $\text{vec}(\mathcal{A}^{(k)}) \leftarrow$  compute and solve equation (8)
10:     $\mathbf{A}_k \leftarrow \text{reshape}(\mathcal{A}^{(k)}, [R_k I_k, R_{k+1}])$ 
11:   end for
12: end while

```

5 Experiments

All experiments were done in MATLAB2017b on a desktop computer with an Intel i5 quad-core processor at 3.2GHz and with 16GB RAM. First, we apply Algorithm 1 for color image completion and demonstrate its efficacy by comparing it to five other state-of-the-art tensor completion algorithms, namely, TNN, HaLRTC, SiLRTC, TMac, and TR-ALS, representing four different approaches towards the completion problem. The TNN method is based on tensor multi-rank and tubal rank [Zhang *et al.*, 2014]. HaLRTC and SiLRTC use the sum of nuclear norms [Liu *et al.*, 2013]. The TMac algorithm [Xu *et al.*, 2015] includes two different schemes, TMac-inc and TMac-dec, depending on different rank adjustment strategies. Here we only compare with TMac-inc as it shows a better performance than TMac-dec in our experiments. The TR-ALS algorithm [Wang *et al.*, 2017] also uses a tensor train of \mathcal{A} but with $R_1 = R_{d+1} > 1$. Moreover, it employs a different ALS for updating each tensor train core, wherein each slice of the core is independently updated, unlike our way of updating the whole core at once. The performance of all methods is measured by their total runtimes and peak signal-to-noise ratio (PSNR) defined as

$$\text{PSNR} = 20 \log_{10}(\text{MAX}_I) - 10 \log_{10}(\text{MSE}),$$

where MAX_I is the maximum possible pixel value and MSE is the mean square error $\|\mathcal{A} - \hat{\mathcal{A}}\|/(n_1 \times n_2 \times 3)$ for a color image of size $n_1 \times n_2$. For an $n_1 \times n_2 \times n_3$ color video, the MSE is the mean square error $\|\mathcal{A} - \hat{\mathcal{A}}\|/(n_1 \times n_2 \times n_3 \times 3)$. The state-of-the-art matrix completion algorithm based on singular value thresholding (SVT) [Cai *et al.*, 2010] was also applied to the examples below, but consistently failed to converge in certain color slices and resulted in PSNR values below 10dB. These poor results also reassure the need of tensor methods for color image and video completion.

Table 1: Best PSNRs and runtimes († TTC time for the same PSNR)

Method	PSNR(dB)	Runtime(s)	TTC Time † (s)
TNN	18.525	48.698	1.469
HaLRTC	18.991	6.788	1.854
SiLRTC	18.804	49.225	1.469
TMac	18.396	10.228	1.469
TR-ALS	20.752	8.559	3.836
TTC	21.074	15.190	—

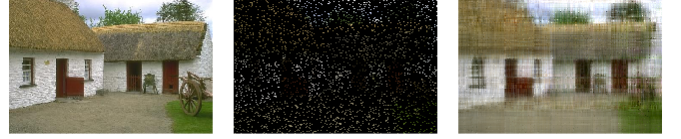


Figure 4: (Left) Original image; (Center) 10% pixels; (Right) Result after 3 TTC ALS iterations PSNR@21.074dB.

5.1 House

As a first application we consider the completion of the house image in the Berkeley Segmentation dataset¹. Only 10% of the $321 \times 481 \times 3$ image was retained, whereby for each missing pixel all color information is removed. Both the TTC and TR-ALS methods are inherently based on tensor trains, and the number of tensor train cores is therefore determined by how the observed tensor is factorized. Appending the $321 \times 481 \times 3$ image \mathcal{V} with zeros to dimensions $324 \times 486 \times 3$ enables a tensor train decomposition of $\text{vec}(\mathcal{V})$ with $I_1 = I_5 = I_6 = 9, I_2 = I_3 = I_4 = 6, I_7 = 3$. The TT-ranks are set to $R_2 = 6, R_3 = R_4 = R_5 = R_6 = 14, R_7 = 3$ for TTC and a uniform value of 7 was used for the TR-ALS. A scaling factor $k = 22$ was used in the initialization of the tensor train. For the TNN, HaLRTC, SiLRTC, and TMac algorithms, the original $341 \times 481 \times 3$ image was used. The performance of the TR-ALS algorithm varied significantly over multiple tests under the same settings due to their random initialization. We therefore ran the TR-ALS algorithm 10 times for each setting and list the average PSNR and runtime. All algorithms were run multiple times for different values of tuning parameters. The best PSNR each algorithm could achieve and their corresponding runtimes are listed in Table 1. The proposed TTC algorithm converges to a PSNR of 21.074dB after 3 ALS iterations (see Figure 4). Moreover, we list the runtimes of TTC to obtain the best PSNR of other algorithms in the rightmost column in Table 1. With a maximum TT-rank of 5, 6, and 9, TTC achieves the PSNR of 18.97dB, 19.63dB, and 20.75dB in 1.469, 1.854, and 3.836 seconds, respectively, with 3 ALS iterations. TR-ALS manages to achieve its best PSNR within 9 seconds, whereas it takes TTC 3.8 seconds to get a better PSNR performance of 20.758dB.

¹<https://www.eecs.berkeley.edu/Research/Projects/CS/vision/bsds/>

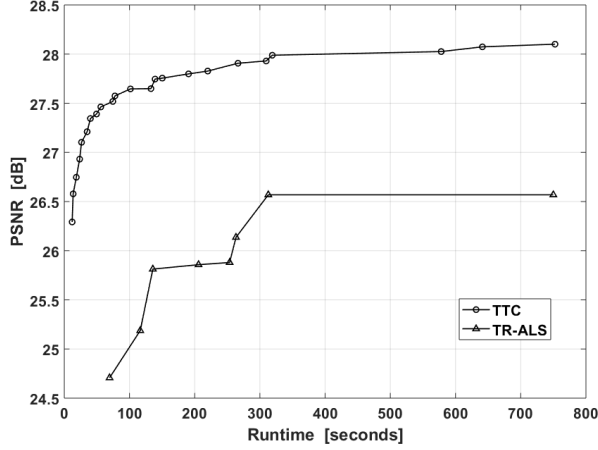


Figure 5: Illustration of best PSNR performances within different runtimes.

5.2 Impression, Sunrise

The performance of the TR-ALS algorithm was very similar to our TTC algorithm in the previous experiment. Here, we use the $931 \times 1200 \times 3$ color picture of Claude Monet’s *Impression, Sunrise* painting to illustrate the scalability of our method. Similarly, we randomly sampled 10% of the image and append the image by zeros to $945 \times 1200 \times 3$. The tensor is factorized into a $9 \times 7 \times 5 \times 3 \times 3 \times 4 \times 4 \times 5 \times 5 \times 3$ tensor thus both the TTC and TR-ALS have ten tensor train cores. Different TT-ranks for both algorithms are tested and the best results are presented. In order to better understand the two algorithms’ convergence rate and performance within different runtimes, we show the results of the experiments in Figures 5 and 6. The TTC algorithm reached a PSNR of 28.101dB when the TT-ranks are set to $R_2 = 5, R_3 = R_4 = R_5 = R_6 = R_7 = R_8 = 20, R_9 = 15, R_{10} = 3$, while TR-ALS converged at 26.569dB. Moreover, it only took the TTC algorithm 13.6 seconds with a maximum TT-rank of 6 to reach the best PSNR that is attainable by TR-ALS after 312.9 seconds and with a uniform TT-rank of 14. We further verify the superiority of the proposed method by comparing the number of parameters needed to reach TR-ALS best performance. For TR-ALS method, due to the uniform high tensor train rank among the cores, there are totally 9408 parameters, while only 1218 parameters are needed in the tensor train completed by the TTC algorithm. Generally, for large scale tensors like high-resolution photos and videos, TTC is superior in speed and storage. In the case of *Impression, Sunrise*, a $23\times$ speedup is demonstrated over TR-ALS with approximately $1/8$ the number of parameters.

5.3 Baseball Pitcher Mariano Rivera

Here we consider a $180 \times 320 \times 80 \times 3$ color video completion experiment with 10% sampled pixels. The 80 frames video clip includes the baseball pitcher Mariano Rivera throwing a baseball, taken from *Mariano Rivera Ultimate Career High-*

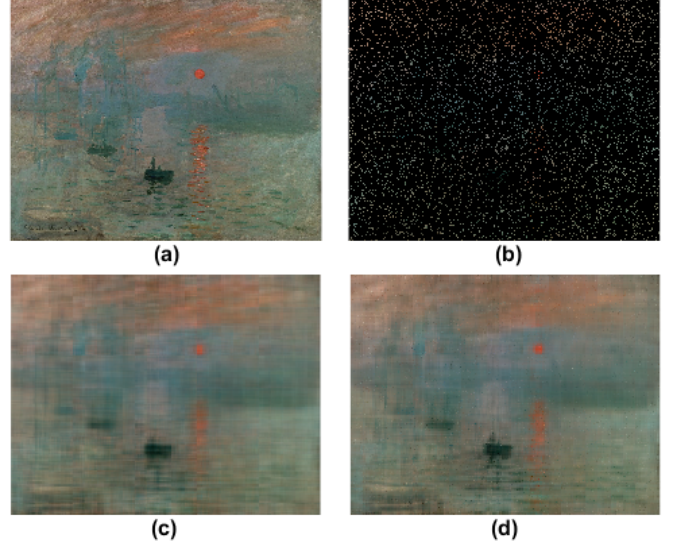


Figure 6: (a) and (b) are the original *Impression, Sunrise* image and the image with 10% pixels observed; (c) is the completed image by TR-ALS with a PSNR of 26.569dB; (d) is the completed image by TTC with a PSNR of 28.101dB.

Table 2: Runtimes of TR-ALS and TTC for different PSNRs

PSNR(dB)	TR-ALS(s)	TTC(s)
17.0	524.81	27.25
18.0	572.71	33.80
19.0	605.81	49.79
20.0	1818.02	193.17
20.5	2492.99	421.03

lights on YouTube². This 4-way tensor is factorized into a $6 \times 6 \times 5 \times 5 \times 4 \times 4 \times 4 \times 4 \times 4 \times 5 \times 3$ tensor. Like before, multiple runs were performed for different TT-ranks in the TR-ALS and TTC methods and the best runtimes are listed in Table 2. We limit the runtimes for both algorithms to under 3000 seconds, thus Table 2 stops at a PSNR of 20.5dB. A uniform TT-rank of 8 is used for TR-ALS to get a PSNR of 20.5dB while for TTC we set the TT-ranks to $R_2 = 6, R_3 = R_4 = R_5 = R_6 = R_7 = R_8 = R_9 = R_{10} = 12, R_{11} = 3$. The table shows that TTC is up to $19\times$ faster than TR-ALS for the same PSNR. Besides the strong expressive power of a tensor train, the superiority of the TTC algorithm also comes from the novel system identification approach that considers every observed entry when progressively updating the cores.

6 Conclusions

We have introduced a novel system identification perspective towards tensor completion where the multi-indices of the known entries act as inputs and their corresponding values act as outputs. The strong expressive power of a tensor train is exploited whose cores are identified via an effective ALS

²<https://www.youtube.com/watch?v=UPtDJuJMyhc>

method. Extensive experiments have shown that the proposed algorithm not only outperforms the state-of-the-art methods in both accuracy and time cost, it is also an economic algorithm in terms of storage requirement.

References

- [Batselier *et al.*, 2017] Kim Batselier, Zhongming Chen, and Ngai Wong. Tensor Network alternating linear scheme for MIMO Volterra system identification. *Automatica*, 84:26–35, 2017.
- [Cai *et al.*, 2010] Jian-Feng Cai, Emmanuel J Candès, and Zuowei Shen. A singular value thresholding algorithm for matrix completion. *SIAM Journal on Optimization*, 20(4):1956–1982, 2010.
- [Candès and Recht, 2009] Emmanuel J Candès and Benjamin Recht. Exact matrix completion via convex optimization. *Foundations of Computational mathematics*, 9(6):717, 2009.
- [Chen, 2015] Yudong Chen. Incoherence-optimal matrix completion. *IEEE Transactions on Information Theory*, 61(5):2909–2923, 2015.
- [Collins and Cohen, 2012] Michael Collins and Shay B Cohen. Tensor decomposition for fast parsing with latent-variable PCFGs. In *Advances in Neural Information Processing Systems*, pages 2519–2527, 2012.
- [Gandy *et al.*, 2011] Silvia Gandy, Benjamin Recht, and Isao Yamada. Tensor completion and low-n-rank tensor recovery via convex optimization. *Inverse Problems*, 27(2):025010, 2011.
- [Grasedyck *et al.*, 2015] Lars Grasedyck, Melanie Kluge, and Sebastian Krämer. Alternating least squares tensor completion in the TT-format. *arXiv preprint arXiv:1509.00311*, 2015.
- [Holtz *et al.*, 2012] S. Holtz, T. Rohwedder, and R. Schneider. The Alternating Linear Scheme for Tensor Optimization in the Tensor Train Format. *SIAM Journal on Scientific Computing*, 34(2):A683–A713, 2012.
- [Kilmer *et al.*, 2013] Misha E Kilmer, Karen Braman, Ning Hao, and Randy C Hoover. Third-order tensors as operators on matrices: A theoretical and computational framework with applications in imaging. *SIAM Journal on Matrix Analysis and Applications*, 34(1):148–172, 2013.
- [Kolda and Bader, 2009] T. Kolda and B. Bader. Tensor Decompositions and Applications. *SIAM Review*, 51(3):455–500, 2009.
- [Kolda *et al.*, 2005] Tamara G Kolda, Brett W Bader, and Joseph P Kenny. Higher-order web link analysis using multilinear algebra. In *Data Mining, Fifth IEEE International Conference on*, pages 8–pp. IEEE, 2005.
- [Kreimer and Sacchi, 2012] Nadia Kreimer and Mauricio D Sacchi. A tensor higher-order singular value decomposition for prestack seismic data noise reduction and interpolation. *Geophysics*, 77(3):V113–V122, 2012.
- [Liu *et al.*, 2013] Ji Liu, Przemyslaw Musialski, Peter Wonka, and Jieping Ye. Tensor completion for estimating missing values in visual data. *IEEE Transactions on Pattern Analysis and Machine Intelligence*, 35(1):208–220, 2013.

- [Mu *et al.*, 2014] Cun Mu, Bo Huang, John Wright, and Donald Goldfarb. Square deal: Lower bounds and improved relaxations for tensor recovery. In *International Conference on Machine Learning*, pages 73–81, 2014.
- [Oseledets, 2011] Ivan V Oseledets. Tensor-train decomposition. *SIAM Journal on Scientific Computing*, 33(5):2295–2317, 2011.
- [Semerci *et al.*, 2014] Oguz Semerci, Ning Hao, Misha E Kilmer, and Eric L Miller. Tensor-based formulation and nuclear norm regularization for multienergy computed tomography. *IEEE Transactions on Image Processing*, 23(4):1678–1693, 2014.
- [Signoretto *et al.*, 2014] Marco Signoretto, Quoc Tran Dinh, Lieven De Lathauwer, and Johan AK Suykens. Learning with tensors: a framework based on convex optimization and spectral regularization. *Machine Learning*, 94(3):303–351, 2014.
- [Tan *et al.*, 2014] Huachun Tan, Bin Cheng, Wuhong Wang, Yu-Jin Zhang, and Bin Ran. Tensor completion via a multi-linear low-n-rank factorization model. *Neurocomputing*, 133:161–169, 2014.
- [Wang *et al.*, 2017] Wenqi Wang, Vaneet Aggarwal, and Shuchin Aeron. Efficient Low Rank Tensor Ring Completion. In *Proceedings of the IEEE Conference on Computer Vision and Pattern Recognition*, pages 5697–5705, 2017.
- [Wen *et al.*, 2012] Zaiwen Wen, Wotao Yin, and Yin Zhang. Solving a low-rank factorization model for matrix completion by a nonlinear successive over-relaxation algorithm. *Mathematical Programming Computation*, pages 1–29, 2012.
- [Xing *et al.*, 2012] Zhengming Xing, Mingyuan Zhou, Alexey Castrodad, Guillermo Sapiro, and Lawrence Carin. Dictionary learning for noisy and incomplete hyperspectral images. *SIAM Journal on Imaging Sciences*, 5(1):33–56, 2012.
- [Xu *et al.*, 2015] Yangyang Xu, Ruru Hao, Wotao Yin, and Zhixun Su. Parallel matrix factorization for low-rank tensor completion. *Inverse Problems & Imaging*, 9(2), 2015.
- [Zhang *et al.*, 2014] Zemin Zhang, Gregory Ely, Shuchin Aeron, Ning Hao, and Misha Kilmer. Novel methods for multilinear data completion and de-noising based on tensor-SVD. In *Proceedings of the IEEE Conference on Computer Vision and Pattern Recognition*, pages 3842–3849, 2014.
- [Zhang *et al.*, 2017] Zheng Zhang, Kim Batselier, Haotian Liu, Luca Daniel, and Ngai Wong. Tensor computation: A new framework for high-dimensional problems in eda. *IEEE Transactions on Computer-Aided Design of Integrated Circuits and Systems*, 36(4):521–536, 2017.
- [Zhou *et al.*, 2017] Tengfei Zhou, Hui Qian, Zebang Shen, Chao Zhang, and Congfu Xu. Tensor Completion with Side Information: A Riemannian Manifold Approach. In *Twenty-Sixth International Joint Conference on Artificial Intelligence*, pages 3539–3545, 2017.